Article

Quantized Cooperative Spectrum Sensing in Bandwidth-Constrained Cognitive V2X Based on Deep Learning

Jingxian Li and Bin-Jie Hu *

School of Electronic & Information Engineering, South China University of Technology,
Guangzhou 510640, China; 201820109914@mail.scut.edu.cn
* Correspondence: eebjiehu@scut.edu.cn

Abstract: The output of the network in a deep learning (DL) based single-user signal detector, which is a normalized 2×1 class score vector, needs to be transmitted to the fusion center (FC) by occupying a large amount of the communication channel (CCH) bandwidth in the cooperative spectrum sensing (CSS). Obviously, in cognitive radio for vehicle to everything (CR-V2X), it is particularly important to propose a method that makes full use of the bandwidth-constrained CCH to obtain the optimal detection performance. In this paper, we firstly propose a novel single-user spectrum sensing method based on modified-ResNeXt in CR-V2X. The simulation results show that our proposed method performs better than two advanced DL based spectrum sensing methods with shorter inference time. We then introduce a quantization-based cooperative spectrum sensing (QBCSS) algorithm based on DL in CR-V2X, and the impact of the number of reported bits on the sensing results is also discussed. Through the experimental results, we conclude that the QBCSS algorithm reaches the optimal detection performance when the number of bits for quantizing local sensing data is 4. Finally, according to the conclusion, a bandwidth-constrained QBCSS scheme based on DL is proposed to make full use of the CCH with limited capacity to achieve the optimal detection performance.

Keywords: CR-V2X; cooperative spectrum sensing; deep learning; quantization; bandwidth-constrained

1. Introduction

Improving road safety has attracted the attention of academia and industry due to the increasing number of vehicles on the road. One potential solution to prevent traffic accidents is to develop safety applications based on vehicle to everything (V2X). In addition, with the development of the social economy, in-vehicle infotainment continues to increase. A rise in the number of applications and services has posed challenges to the limited spectrum resources that have been allocated to V2X [1].

Cognitive radio (CR) is an efficient technology to alleviate spectrum scarcity. It enables unauthorized/secondary user (SU) to utilize the underused spectrum resources, provided that they do not cause harmful interference to the authorized/primary user (PU). To realize CR technology in V2X, cognitive radio for V2X (CR-V2X) has been proposed [2]. CR-enabled vehicles can opportunistically access additional licensed spectrum, for example, TV whitespace spectrum, according to the quality-of-service requirements of the applications [1]. As a key component of identifying idle licensed spectrum in CR systems, spectrum sensing is vital to CR-V2X.

Spectrum sensing which has been fully studied in conventional CR networks [3] is still in the development stage in CR-V2X. Due to a series of effects brought by the high-speed movement of vehicles, CR-V2X has its unique features compared with the conventional static CR networks, such as the fluctuation of wireless communication channels over time and space, the dynamics of the network topology and diverse environments where the network is located [1,4].

There are three main conventional CR-V2X spectrum sensing technologies—including energy detection, cyclostationary feature detection, and matched filter detection. Energy detection is widely used in CR-V2X due to its simplicity and no need for prior knowledge of the PU signal [5,6]. To judge the existence of the PU, the energy detector compares the strength of the received signal with a predetermined threshold [7]. However, the energy detector fails to work when the signal to noise ratio (SNR) is low, which is known as the SNR-wall [8]. Cyclostationary feature detection exploits the periodicity of the correlation of the modulated signal, which can distinguish PU signal from noise signal because the PU signal is a kind of modulated signal while the noise is not [9,10]. In addition, a detector-based on cyclostationary feature which can detect a PU signal in low SNR and identify the type of modulation signal. Nevertheless, this detection technique is not widely used in CR-V2X because of its need for prior knowledge of the PU signal and complex calculation of the spectral correlation function [2]. Compared with energy detection and cyclostationary feature detection, matched filter detection performs best due to its perfect knowledge of PU signal features in advance [11]. However, techniques based on the matched filter are usually aimed at scenarios where the PU signal is deterministic. The inaccurate demodulated relevant information which is stored in the SU database in advance will greatly deteriorate the detection performance. Therefore, matched filter detector is hardly applied to CR-V2X.

As the essence of spectrum sensing is a binary classification problem. Recently, deep learning (DL) for spectrum sensing has gained remarkable performance in conventional CR networks. The authors in [12] employ a convolution neural network (CNN) to solve spectrum sensing. They used the pre-processed cyclostationary feature and energy feature extracted from the presence of the PU signal and the presence of only the noise signal to train the CNN model to achieve higher detection probability than cyclostationary feature detection. To explore the data-driven test statistic for spectrum sensing, Liu et al. [13] introduced a deep neural network (DNN)-based detection framework. They used the sample covariance matrix as the input of a CNN, and analyzed the theoretical performance of CNN-based methods for the first time. One kind of CNN model for spectrum sensing tasks considered in [14] is the residual network (ResNet) model. To overcome the problem of noise power uncertainty, they normalized the power of sample and used the power spectrum as the input of ResNet, which showed better performance than the maximum–minimum eigenvalue ratio-based method and frequency domain entropy-based method. Inspired by the result of [15] where convolutional long short-term deep neural networks (CLDNN) performs best in modulation recognition tasks, a deep learning based detector using CLDNN is proposed in [16], which is applicable for arbitrary types of PU signals with no additional information of the signal. Given that the sensing result of individual SUs is susceptible to errors due to the hidden PU problem, a novel DNN-based cooperative spectrum sensing (CSS) scheme which is named as deep cooperative sensing (DCS) is proposed in [17]. It can autonomously learn from training samples of distributed sensing nodes to obtain the optimal CSS strategy. Unlike DCS, a DL based cooperative detection system named 'SoftCombinationNet' is proposed to exploit the soft information from distributed sensing nodes [16]. All the above papers deduced that DL technology performs the task of spectrum sensing better as compared to the conventional sensing methods in static CR networks.

Unlike the conventional CSS system where a specific fusion rule is adopted to combine the decision information from the distributed nodes, that the 'SoftCombinationNet' proposed in [16] can directly learn the best fusion rule through training and provide substantial performance gain over conventional CSS methods. Unfortunately, because what is sent to the fusion center (FC) through the communication channel (CCH) is the score vector of two hypotheses about PU signal obtained by the local DL based spectrum sensing method, it will pose a huge challenge for V2X with bandwidth-constrained CCH. As the CR-V2X system can only tolerate low transmitting overhead, it is necessary to compress the result derived by the single-user spectrum sensing based on the DL algorithm before transmitting

to the FC. Motivated by the conclusion obtained in [16,18], in this paper, we propose a bandwidth-constrained quantization-based cooperative spectrum sensing (QBCSS) scheme based on DL. The major contributions of this paper can be summarized as follows:

(1)   We propose a novel single-user spectrum sensing based on modified-ResNeXt in CR-V2X, which shows better detection performance than two advanced DL based spectrum sensing methods as mentioned above [14,16] and decent generalization ability for different vehicle velocities.

(2)   Based on the SoftCombinationNet proposed in [16], we study how many bits should be reported in QBCSS to achieve detection performance close to that of spectrum sensing with raw sensing results. Through simulation results, we conclude that only four bits of QBCSS are needed to achieve the optimal detection performance.

(3)   According to the conclusion drawn in (2), considering the bandwidth-constrained CCH in CR-V2X, we propose a bandwidth-constrained QBCSS scheme to make full use of the CCH with limited capacity to achieve the best detection performance.

The rest of this paper is organized as follows. In Section 2, we describe the system model. The single-user spectrum sensing scheme based on modified-ResNeXt in CR-V2X and simulation results of the proposed algorithm are provided in Section 3. The proposed QBCSS based on SoftCombinationNet is introduced in Section 4, and we also provide the simulation results in this section. Section 5 concludes the paper.

2. System Model

We consider a CR-V2X system consisting of one PU and B cognitive vehicles equipped with CR devices. For the sake of simplicity, we assume that the vehicles are moving with a constant velocity v. To avoid wasting resources, only when the currently available spectrum resources cannot meet the communication requirements of the system, the vehicle will enable the CR device to search for an idle licensed frequency band to transmit data. The PU signal transmitter will transmit the PU signal on the authorized frequency band when it is occupied. The SU performs spectrum sensing based on the sample values on the frequency band of interest. The PU signal detection at the SU can be modeled as the following binary hypothesis testing problem [19]

$$x(t) = \begin{cases} n(t), & H_0 \\ h(t)s(t) + n(t), & H_1 \end{cases}, \tag{1}$$

where $x(t)$ is the signal received by the SU, $s(t)$ is the signal transmitted by the PU, $n(t)$ is a zero-mean additive white Gaussian noise (AWGN) with a variance σ_n^2, $h(t)$ is the sensing channel gain between the PU and the SU. The power attenuation $g(t)$ from transmitter to receiver is given by

$$g(t) = |h(t)|^2 = \beta(d(t)) \cdot \varphi \cdot \alpha, \tag{2}$$

where $d(t)$ is the distance between the PU and SU at time t, then the path-loss is $\beta(d(t))$. φ and α are the shadowing fading component and multipath fading component. Also, H_0 and H_1 are the two hypotheses denoting the absence and presence of PU in a certain band respectively. Obviously, the problem shown in (1) can be viewed as a classification problem with two categories. One of the categories is D_0, which means that the sensing result of the SU is that the licensed frequency band to be detected is idle, so the SU can access it. The other category is D_1, which means that the sensing result of the SU is that the licensed frequency band to be detected is being occupied, so the SU cannot access it. Like the measurement indicators used in [14,16], we also use the probability of detection P_d and the probability of false alarm P_f to measure the performance of the spectrum sensing algorithm, which are defined as

$$\begin{aligned} P_d &= P(D_1|H_1), \\ P_f &= P(D_1|H_0). \end{aligned} \tag{3}$$

The values obtained by the cognitive vehicle sampling the modulated signal propagated through the fading channel in the CR-V2X scenario can be written as

$$\boldsymbol{x} = [x_1, x_2, \cdots, x_i, \cdots x_N],\tag{4}$$

where x_i represents the i-th sample value of received time domain complex signal $\boldsymbol{x}$, N represents the sample length of the received signal. To enhance the generalization ability of the sensing model, energy normalization is performed prior to training or inferring. Then, the sample value after energy normalization can be expressed as

$$\boldsymbol{x}' = \frac{\boldsymbol{x}}{\sqrt{energy_{\boldsymbol{x}}}},\tag{5}$$

where $energy_{\boldsymbol{x}} = \sum_{i=1}^{N}|x_i|^2$. Therefore, the processed dataset $\boldsymbol{y}$ that is to be fed into the deep learning model can be written as

$$\boldsymbol{y} = \left\{ (\boldsymbol{x}'_1, b_1), (\boldsymbol{x}'_2, b_2), \cdots, (\boldsymbol{x}'_k, b_k), \cdots (\boldsymbol{x}'_K, b_K) \right\},\tag{6}$$

where x_k denotes the k-th sample of the dataset after energy normalization, K denotes the size of the dataset, b_k denotes the label corresponding to the k-th sample of the dataset. The value of b_k is either 0 or 1. When the hypothesis is H_0, $b_k = 0$, and when the hypothesis is H_1, $b_k = 1$. Furthermore, to facilitate the calculation of cross entropy, we use a one-hot vector to represent the label b_k as

$$b_k = \left\{ \begin{array}{ll} [0\ 1], & H_0 \\ [1\ 0], & H_1 \end{array} \right. .\tag{7}$$

Finally, the output of the DL model is a 2×1 class score vector [20], which can be written as

$$p_\theta(\boldsymbol{x}'_k) = \left[\begin{array}{c} p_{\theta|H_0}(\boldsymbol{x}'_k) \\ p_{\theta|H_1}(\boldsymbol{x}'_k) \end{array} \right],\tag{8}$$

with

$$p_{\theta|H_0}(\boldsymbol{x}'_k) + p_{\theta|H_1}(\boldsymbol{x}'_k) = 1.\tag{9}$$

where θ denotes the parameter of the DL model, and $p_\theta(\cdot)$ denotes the expression of the entire model. The training process of the model is to find the optimal solution θ^* of θ which satisfies [20]

$$\theta^* = arg\ \max_\theta H(\theta),\tag{10}$$

where $H(\theta) = \prod_{k=1}^{K} p_{\theta|H_0}(\boldsymbol{x}'_k)^{1-b_k} p_{\theta|H_1}(\boldsymbol{x}'_k)^{b_k}$, and we adopt the cross-entropy loss function [17] in this paper, which can be written as

$$L(\theta) = -\sum_{k=1}^{K} b_k log p_\theta(\boldsymbol{x}'_k) + (1 - b_k) log(1 - p_\theta(\boldsymbol{x}'_k)).\tag{11}$$

The smaller the value of $L(\theta)$, the closer the predicted label is to the actual label and the better the performance of the model. In this case, when the $p_\theta(\boldsymbol{x}'_k)$ satisfies

$$p_{\theta|H_0}(\boldsymbol{x}'_k) > p_{\theta|H_1}(\boldsymbol{x}'_k),\tag{12}$$

the final decision made by the model is D_0, otherwise the decision is D_1.

3. Single-User Spectrum Sensing Based on Modified-ResNeXt in CR-V2Xs

3.1. Network Architecture

Inspired by the result of [21] where ResNeXt performs well on the ILSVRC 2016 classification task, we also adopt this kind of architecture in this paper. Compared with ResNet, ResNeXt inherits the idea of ResNet while incorporating the idea of split-transform-

merge of Inception network [22], so the classification effect is naturally better than ResNet. When the basic building blocks of ResNet have the same complexity as the basic building blocks of ResNeXt, the accuracy of the network adopting the basic building blocks of ResNeXt is higher [21]. The basic modified-ResNeXt module whose cardinality is 4 is considered in this paper, as shown in Figure 1. Based on the basic building module, the details of the modified-ResNeXt structure constructed in this paper is shown in Table 1, where 'MaxPool1D' denotes the one-dimensional max-pooling layer, 'AvgPool1D' denotes the one-dimensional average pooling, 'Fc' denotes the fully connected layer. The first parameter in the pooling layer represents the pooling size, the second parameter represents the type of pooling, that is, max-pooling or average-pooling, the third parameter represents the step size of pooling, the last two parameters 'S' and 'F' have the same meaning as the convolutional layer. As for the fully connected layer, the first parameter represents the number of nodes and the last parameter represents the activation function.
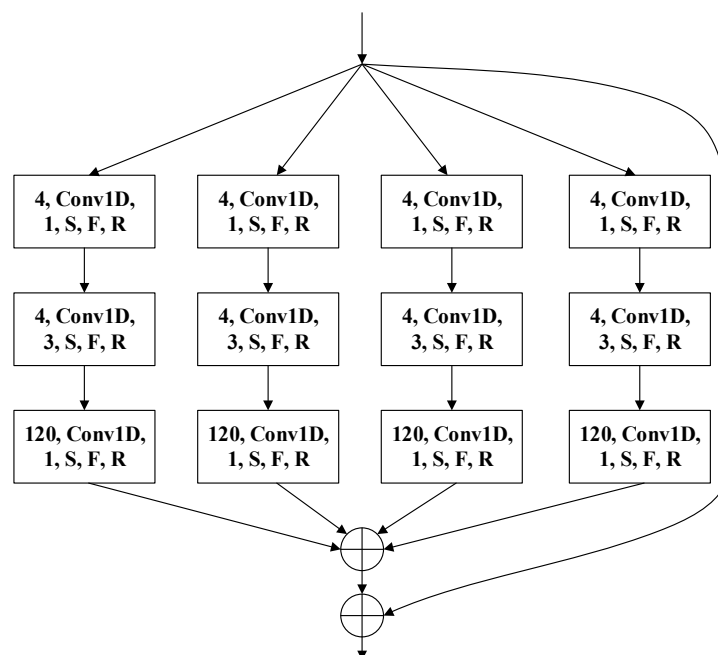
Figure 1. Basic modified-ResNeXt module, where the first parameter denotes the number of convolutional kernels, the second parameter 'Conv1D' denotes the one-dimensional convolutional layer, the third parameter denotes the size of convolutional kernels, the fourth parameter 'S' denotes padding to the same size, the fifth parameter 'F' denotes channel order of the input data immediately follows the batch, the last parameter 'R' denotes Relu activation function.

Table 1. Structure of proposed modified-ResNeXt.

Index	Layer
1	48, Conv1D, 15, S, F, R
2	60, Conv1D, 7, S, F, R
3	3, MaxPool1D, 2, S, F
4	basic modified-ResNeXt module
5	32, AvgPool1D, 1, S, F
6	Flattern
7	32, Fc, Relu
8	Dropout (0.2)
9	2, Fc, Softmax

3.2. Dataset Generation

For the dataset, we use MATLAB to generate the modulated signal whose modulation mode is BPSK, and the SNR ranges from -20 dB to 20 dB with an interval of 1 dB. The modulated signal is sampled with the length of 1024 after propagating through the V2X channel under urban and highway environments as described in [23,24]. The number of samples for each SNR is 1000, so the final dataset size is $40000 \times 2 \times 1024$, where 2 denotes every point is a complex number, which can be divided into real and imaginary parts. Then the entire dataset is partitioned into three different sets for training, validation, and testing with a commonly used split ratio of 3:1:1. To verify the generalization ability of the model, we also test the detection performance of a well-trained network over signals with different vehicle velocities from the training signals.

3.3. Simulation Results

In this section, extensive simulation results are provided to demonstrate the performance of the proposed model. Also, the impact of vehicle velocity is investigated. Considering the constant false alarm rate detector, we use the customized two-stage training strategy proposed in [16].

3.3.1. Comparison with Different Models

Figure 2 compares the detection performance of the proposed model with three other models, namely ResNet [14], DetectNet [16], and conventional energy detection. Considering that under high SNR (here refers to greater than -4 dB), the detection probability of various algorithms has reached the maximum value of 1, so only the part in the range of -20 dB to -4 dB is shown in Figure 2. It can be observed that the detection performance of any spectrum sensing algorithm based on DL is much better than that of conventional energy detection, especially in low SNR, the detection performance gap between them is more obvious. The value of P_d in our proposed model reaches 97% at -13 dB with lower P_f, which is 5% higher than that of ResNet and 9% higher than that of DetectNet under urban environment. In addition to detection performance, we also compare the inference time of our proposed model with ResNet and DetectNet, as shown in Figure 3. It can be seen that, no matter what kind of V2X communication environment, the model proposed in this paper with the shortest inference time outperforms two other DL models, which is vital for the latency-sensitive V2X. Furthermore, the number of parameters, model size and floating point of operations (FLOPs) of various DL models are compared in Table 2. It is not difficult to find that the parameter quantity of the model proposed in this paper is about one order of magnitude smaller than that of ResNet and three orders of magnitude smaller than that of DetectNet. Besides, the capacity of storage space required by our proposed model is about one-thousandth of that required by DetectNet, and is less than one-fifth of that required by ResNet. Moreover, the FLOPs required by our proposed model are about one order of magnitude smaller than that of ResNet and two orders smaller than that of DetectNet. Therefore, the proposed algorithm can not only guarantee detection performance but also effectively shorten sensing time, saving a certain capacity of storage space and computing resources in CR-V2X.

Table 2. Comparison of attributes different deep learning models. The attributes involved in the comparison are parameter amount, model size, and FLOPs.

| Model	Parameter Amount	Model Size (MB)	FLOPs
DetectNet	6.4×10^7	728.96	1.3×10^8
ResNet	3.9×10^5	4.71	9.4×10^6
modified-ResNeXt	6.3×10^4	0.88	1.2×10^6
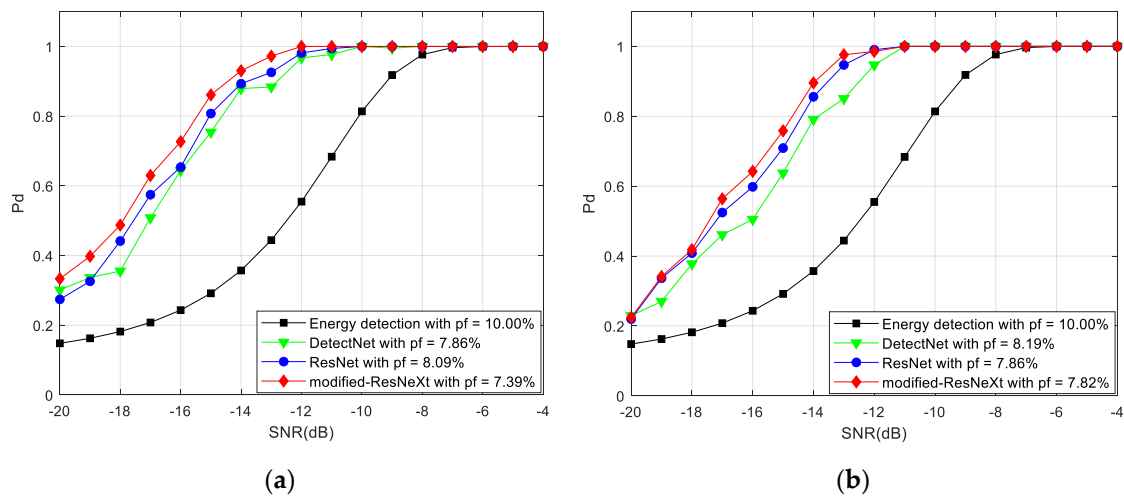
Figure 2. Detection performance of various algorithms. (**a**) Detection performance under urban environment; (**b**) Detection performance under highway environment.
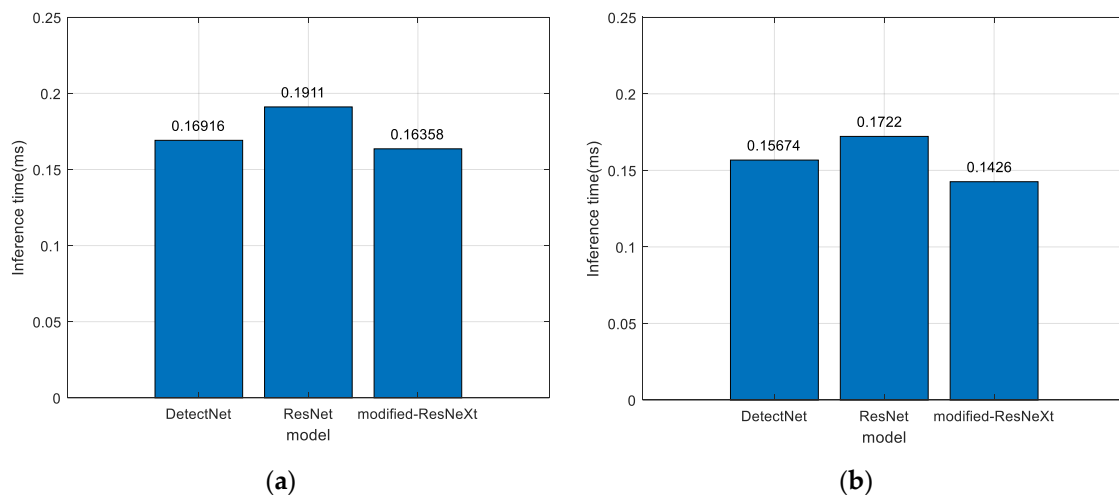
Figure 3. Inference time of various deep learning models. (**a**) Inference time under urban environment; (**b**) Inference time under highway environment.

3.3.2. Impact of Vehicle Velocity

Figure 4 illustrates the generalization ability of our proposed model. In particular, we test the detection performance of a well-trained network over signals with different vehicle velocities under urban and highway environments. As can be observed, the modified-ResNeXt provides decent generalization under these two environments. Furthermore, as the vehicle speed increases, the detection performance of modified-ResNeXt under urban environment gradually decreases. This is because the higher the vehicle speed, the faster the channel conditions fluctuate, and the more severe the signal fading. However, under the highway environment, the vehicle speed is already high enough, so the overall detection performance of the system has stabilized as the vehicle speed increases.
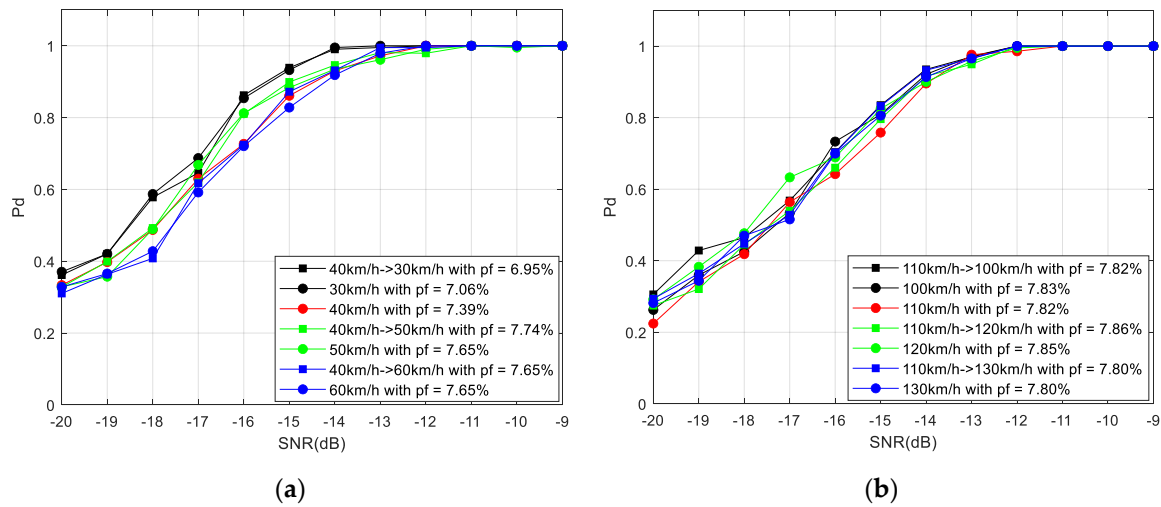
Figure 4. Generalization ability to different velocities, where "a km/h->b km/h" denotes signals at a speed of b km/h to be tested in a well-trained network over signals at a speed of a km/h. (**a**) Detection performance under urban environment; (**b**) Detection performance under highway environment.

4. Quantized Cooperative Spectrum Sensing Based on Deep Learning

4.1. Quantized Collaboration Scheme Based on Deep Learning

4.1.1. Quantification Process

In the CR-V2X system, the sensing result obtained by cognitive vehicles in CSS is transmitted to the FC through the vehicle CCH. Take the V2X as an example, when the CCH is 10 MHz, the modulation is QPSK and the coding rate is 0.57, the number of Resource Block (RB) is 50 in one subframe interval [25]. In this paper, we assume that the total number of RBs that can be used to transmit sensing result of cognitive vehicles participating in CSS is L, and the number of information bit of each RB used to transmit sensing result of cognitive vehicles is one to reduce the overhead caused by CSS. Therefore, for each cognitive vehicle participating in CSS, they transmit sensing result at the same subframe time, and the FC receives the sensing information from neighboring vehicles at the same time. For the sake of simplicity, the number of RBs is replaced by the number of information bits in the following, and the RBs in vehicle CCH are evenly allocated to each cognitive vehicle participating in CSS. Then, the total number of information bits M allocated to quantify local sensing result satisfies

$$M \leq L/B. \tag{13}$$

Therefore, the local sensing result $p_\theta(x'_k)$ obtained by the single-user neural network has a total of 2^M values after quantization, and the number of quantization intervals thus obtained is 2^M. The quantization threshold vector t is given by

$$t = \left[0, \frac{1}{2^M}, \frac{2}{2^M}, \cdots \frac{2^M - 1}{2^M}, 1\right]. \tag{14}$$

Then, the local sensing result $p_\theta(x'_k)$ obtained by the j-th cognitive vehicle participating in CSS can be coded as D_j uploading to the FC through the CCH according to the following quantizer

$$D_j = \begin{cases} \underbrace{00\cdots00}_{M\ in\ tatal}, & 0 \le p_{\theta|H_0}(x'_k) \le \dfrac{1}{2^M} \\[2ex] \underbrace{00\cdots01}_{M\ in\ tatal}, & \dfrac{1}{2^M} < p_{\theta|H_0}(x'_k) \le \dfrac{2}{2^M} \\[2ex] \qquad\vdots \\[2ex] \underbrace{11\cdots10}_{M\ in\ tatal}, & \dfrac{2^M-2}{2^M} < p_{\theta|H_0}(x'_k) \le \dfrac{2^M-1}{2^M} \\[2ex] \underbrace{11\cdots11}_{M\ in\ tatal}, & \dfrac{2^M-1}{2^M} < p_{\theta|H_0}(x'_k) \le 1 \end{cases}. \tag{15}$$

After the FC receives the data from the cognitive vehicle participating in CSS, it adopts the *random* function to decode the data into $p'_\theta(x'_k)$ as the following dequantizer

$$p'_\theta(x'_k) = \begin{cases} \begin{bmatrix} p'_{\theta|H_0}(x'_k) = random\left(0, \dfrac{1}{2^M}\right) \\ 1 - p'_{\theta|H_0}(x'_k) \end{bmatrix}, & \underbrace{00\cdots00}_{M\ in\ tatal} \\[3ex] \begin{bmatrix} p'_{\theta|H_0}(x'_k) = random\left(\dfrac{1}{2^M}, \dfrac{2}{2^M}\right) \\ 1 - p'_{\theta|H_0}(x'_k) \end{bmatrix}, & \underbrace{00\cdots01}_{M\ in\ tatal} \\[3ex] \qquad\qquad\vdots \\[3ex] \begin{bmatrix} p'_{\theta|H_0}(x'_k) = random\left(\dfrac{2^M-2}{2^M}, \dfrac{2^M-1}{2^M}\right) \\ 1 - p'_{\theta|H_0}(x'_k) \end{bmatrix}, & \underbrace{11\cdots10}_{M\ in\ tatal} \\[3ex] \begin{bmatrix} p'_{\theta|H_0}(x'_k) = random\left(\dfrac{2^M-1}{2^M}, 1\right) \\ 1 - p'_{\theta|H_0}(x'_k) \end{bmatrix}, & \underbrace{11\cdots11}_{M\ in\ tatal} \end{cases}. \tag{16}$$

Finally, $p'_\theta(x'_k)$ is sent to SoftCombinationNet for training.

4.1.2. Simulation Results and Discussions

Figure 5 depicts the detection performance of QBCSS with different bits of quantized information. For illustration purpose, the Logical-OR (LO) rule is used in the conventional cooperative detection scheme, since it in general yields the highest P_d. Comparing the performance of 'SoftCombinationNet' (SCN) and LO, we find that these two curves are very close at high SNR. Also, it is obvious that the detection performance of single-node spectrum sensing is much worse than that of CSS. This is because CSS effectively utilizes the spatial diversity of distributed sensing nodes. Furthermore, the more quantized information bits obtained by the single-user, the better the QBCSS performs. Due to the excessive randomness of ONBSCN, the quantization scheme with one-bit of information is not considered in practical applications. However, when the number of quantized information bits of the local spectrum sensing result is 4, the detection performance of the QBCSS is very close to that of SCN which is of no quantization. Taking the limited resources of the vehicle CCH into account, more quantized information bits are meaningless, and the saved CCH capacity can be used for the transmission of other vehicle information. Therefore, it can be concluded that when the number of quantized information bits of the local spectrum sensing result is 4, the detection performance of QBCSS is optimal.
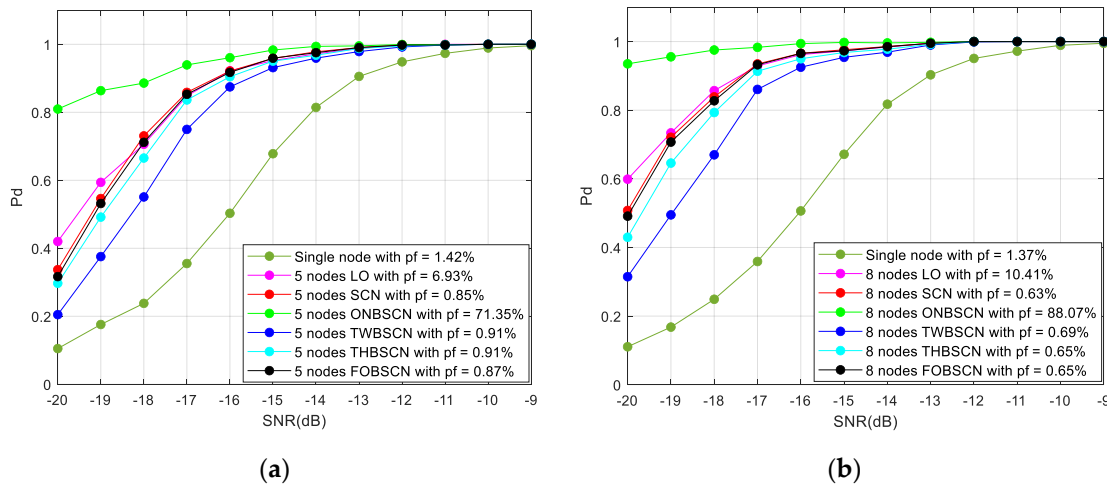
Figure 5. Detection performance of QBCSS over different quantized information bits. (**a**) Five-node QBCSS; (**b**) eight-node QBCSS. Where "ONBSCN" represents one-bit quantization, "TWBSCN" represents two-bit quantization, "THBSCN" represents three-bit quantization and "FOBSCN" represents four-bit quantization.

4.2. Bandwidth-Constrained Quantized Collaboration Scheme Based on Deep Learning

The bandwidth-constrained quantized collaboration scheme based on DL in this paper requires pre-stored data in the database, which are the combinations of the number of the cognitive vehicle that actually participate in CSS and their quantized information bits of the local spectrum sensing results. Given the upper limit of the bandwidth of the vehicle CCH, for the sake of simplicity, we assume that the total number of bits of information used by the vehicles to transmit the sensing result is L, the number of the cognitive vehicle that can participate in CSS is B, the number of the cognitive vehicle that actually participates in CSS is b and the number of quantized information bits of the local spectrum sensing results allocated to each cognitive vehicle participating in CSS is m. Then, for a given pair of $\{B, L\}$, combined with the discussion in Section 4.1.2, the optimal combination scheme can be seen as the answer to the optimization

$$
\begin{aligned}
[b^*, m^*] &= \underset{(b,m)}{\operatorname{argmax}} P_d^{(B,L)}(b, m) \\
&s.t.\ C1 : 0 \leq bm \leq L \\
&\qquad C2 : 0 \leq m \leq 4 \\
&\qquad C3 : b, m \in N^*
\end{aligned}
, \tag{17}
$$

where $P_d^{(B,L)}(b, m)$ represents the detection probability corresponding to each combination under the aforementioned assumptions.

The optimal solution to (17) can be easily obtained by a discrete search along with both b and m. Consequently, the algorithm for finding $\{b^*, m^*\}$ is given as Algorithm 1.

Algorithm 1 Enumeration method to find {*b,m*}

Initialize $P_d^* = 0$, $\underset{(b,m)}{\text{argmax}}P_d^{(1,L)}(b,m) = (1,1)$

for $i = 2, \cdots B$ **do**

if $i \leq L$

$$\underset{(b,m)}{\text{argmax}}P_d^{(i,L)}(b,m) = \underset{(b,m)}{\text{argmax}}P_d^{(i-1,L)}(b,m)$$

for $j = 1, \cdots 4$ **do**

if $ij \geq L$

$$j - -$$

if $P_d^{(i,L)}(i,j) > P_d^*$? **then**

$$P_d^* = P_d^{(i,L)}(i,j)$$
$$[b^*, m^*] = [i,j]$$

End if
End if
End for
End if
End for

Thus, based on the prepared database, the process of the QBCSS in bandwidth-constrained CR-V2Xs based on DL can be described as Algorithm 2.

Algorithm 2 QBCSS in bandwidth-constrained CR-V2Xs based on DL

01: The FC confirms the capacity of the CCH and the number of vehicles that can participate in CSS
02: The FC select the optimal solution from the database based on the information obtained in the first step
03: The FC notifies vehicles that need to participate in CSS based on the location of the vehicle
04: The notified vehicle performs local spectrum sensing
05: The cognitive vehicles upload the quantified local spectrum sensing results to the FC
06: The FC dequantizes the received quantitative information to restore the class score vector
07: The FC makes the final decision

It should be noted that the third step is to select the vehicle closest to the PU based on the location.

4.3. Simulation Results

In this section, we assume that $L = 10$ and $B = 10$. Then, the candidate optimal combination schemes found through the enumeration method are shown in Table 3.
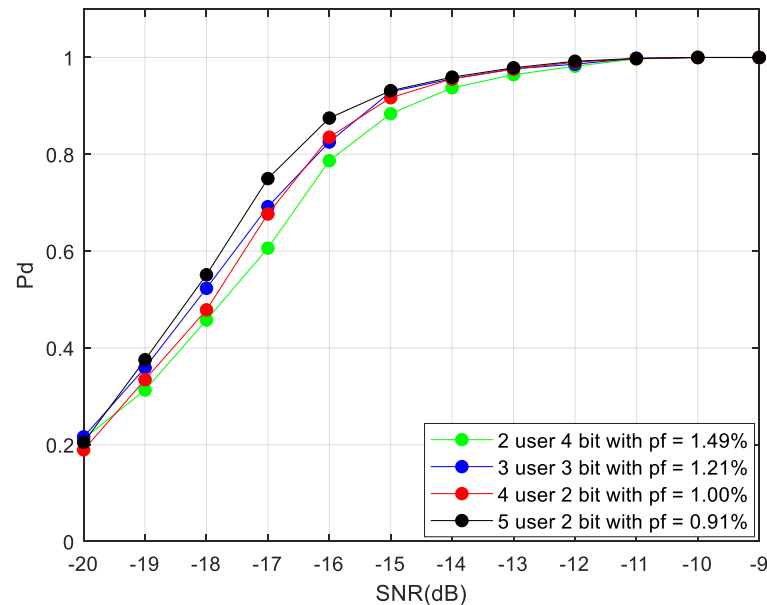
Table 3. Candidate optimal combination scheme.

Number of Vehicles Participating in CSS	Number of Quantified Information Bits
2	4
3	3
4	2
5	2

In Figure 6, we compare the detection performance of the combination scheme shown in Table 3. It can be observed that the CSS performs best when the number of vehicles participating in CSS is 5 and the number of quantized information bits of the local spectrum sensing results allocated to each vehicle participating in CSS is 2. At the same time, it can be observed that the higher the utilization rate of the bandwidth-constrained CCH, the better the detection performance of the system. Furthermore, when the total number of bits

of information reported by vehicles is the same in the two combination schemes, the more vehicles participating in the CSS, the better the detection performance. This is consistent with our purpose of introducing cooperation.

Figure 6. Detection performance of the candidate optimal combination scheme. Where 'a user b bit' means the number of cognitive vehicles is 'a' and the number of quantified information bits is 'b'.

5. Conclusions

In this paper, we first propose a DL based single-user spectrum sensing model called modified-ResNeXt in CR-V2Xs. It shows an improvement in detection performance than two other well-performing algorithms, that is ResNet and DetectNet. Specifically, when the SNR equals -13 dB under urban environment, the P_d of the proposed model is 5% higher than that of ResNet and 9% higher than that of DetectNet, but with lower P_f, shorter inference time, smaller model size. Also, the DL based detector provides decent generalization over signals with different vehicle velocities under urban and highway environment. Then, taking the upper limit of the bandwidth of the vehicle CCH into account, we discuss how many bits should be reported in QBCSS based on DL, and conclude that when the number of quantized information bits of the local spectrum sensing result is 4, the detection performance achieves optimal. Based on this conclusion, a bandwidth-constrained quantized collaboration scheme based on DL is proposed to make full use of the CCH with limited capacity to achieve optimal detection performance.

Author Contributions: Conceptualization, J.L.; Methodology, J.L.; Software, J.L.; Validation, J.L.; Formal analysis, J.L.; Investigation, J.L.; Resources, B.-J.H.; Data curation, J.L.; Writing—original draft preparation, J.L.; Writing—review and editing, B.-J.H.; Visualization, J.L.; Supervision, B.-J.H.; Project administration, B.-J.H.; Funding acquisition, B.-J.H. All authors have read and agreed to the published version of the manuscript.

Conflicts of Interest: The authors declare no conflict of interest.

References

1. Singh, K.D.; Rawat, P.; Bonnin, J. Cognitive radio for vehicular ad hoc networks (CR-V2Xs): Approaches and challenges. *EURASIP J. Wirel. Commun. Netw.* **2014**, *2014*, 49. [CrossRef]
2. Chembe, C.; Noor, R.M.; Ahmedy, I.; Oche, M.; Kunda, D.; Liu, C.H. Spectrum sensing in cognitive vehicular network: State-of-Art, challenges and open issues. *Comput. Commun.* **2017**, *97*, 15–30. [CrossRef]
3. Yucek, T.; Arslan, H. A survey of spectrum sensing algorithms for cognitive radio applications. *IEEE Commun. Surv. Tutor.* **2009**, *11*, 116–130. [CrossRef]
4. Felice, M.D.; Doost-Mohammady, R.; Chowdhury, K.R.; Bononi, L. Smart radios for smart vehicles: Cognitive vehicular networks. *IEEE Veh. Technol. Mag.* **2012**, *7*, 26–33. [CrossRef]
5. Qian, X.; Hao, L. Spectrum Sensing with Energy Detection in Cognitive Vehicular ad hoc Networks. In Proceedings of the 2014 IEEE 6th International Symposium on Wireless Vehicular Communications, Vancouver, BC, Canada, 14–15 September 2014; pp. 1–5.
6. Piran, M.J.; Cho, Y.; Yun, J.; Ali, A.; Suh, D.Y. Cognitive radio-based vehicular ad hoc and sensor networks. *Int. J. Dist. Sens. Netw.* **2014**, *2*, 4–17.
7. Urkowitz, H. Energy detection of unknown deterministic signals. *Proc. IEEE* **1967**, *29*, 523–531. [CrossRef]
8. Tandra, R.; Sahai, A. SNR walls for signal detection. *IEEE J. Sel. Top. Signal Process.* **2008**, *2*, 4–17. [CrossRef]
9. Gardner, W.A. Spectral correlation of modulated signals: Part I—Analog modulation. *IEEE Trans. Commun.* **1987**, *35*, 584–594. [CrossRef]
10. Gardner, W.A.; Brown, W.A.; Chen, C.K. Spectral correlation of modulated signals: Part II—Digital modulation. *IEEE Trans. Commun.* **1987**, *35*, 595–601. [CrossRef]
11. Kabeel, A.A.; Hussein, A.H.; Khalaf, A.A.M.; Hamed, H.F.A. A Utilization of multiple antenna elements for matched filter based spectrum sensing performance enhancement in cognitive radio system. *AEU Int. J. Electron. Commun.* **2019**, *107*, 98–109. [CrossRef]
12. Han, D.; Sobabe, G.C.; Zhang, C.; Bai, X.; Wang, Z.; Liu, S.; Guo, B. Spectrum Sensing for Cognitive Radio Based on Convolution Neural Network. In Proceedings of the 2017 10th International Congress on Image and Signal Processing, BioMedical Engineering and Informatics (CISP-BMEI), Shanghai, China, 14–16 October 2017; pp. 1–6.
13. Liu, C.; Wang, J.; Liua, X.; Liang, Y. Deep CM-CNN for spectrum sensing in cognitive radio. *IEEE J. Sel. Areas Commun.* **2019**, *37*, 2306–2321. [CrossRef]
14. Zheng, S.; Chen, S.; Qi, P.; Zhou, H.; Yang, X. Spectrum sensing based on deep learning classification for cognitive radios. *China Commun. Lett.* **2020**, *17*, 138–148. [CrossRef]
15. West, N.E.; O'Shea, T. Deep Architectures for Modulation Recognition. In Proceedings of the 2017 IEEE International Symposium on Dynamic Spectrum Access Networks (DySPAN), Baltimore, MD, USA, 6–9 March 2017; pp. 1–6.
16. Gao, J.; Yi, X.; Zhong, C.; Chen, X.; Zhang, Z. Deep learning for spectrum sensing. *IEEE Wirel. Commun. Lett.* **2019**, *8*, 1727–1730. [CrossRef]
17. Lee, W.; Kim, M.; Cho, D.H. Deep cooperative sensing: Cooperative spectrum sensing based on convolutional neural networks. *IEEE Trans. Veh. Technol.* **2019**, *68*, 3005–3009. [CrossRef]
18. Nguyen-Thanh, N.; Ciblat, P.; Maleki, S.; Nguyen, V.-T. How many bits should be reported in quantized cooperative spectrum sensing? *IEEE Wirel. Commun. Lett.* **2015**, *4*, 465–468. [CrossRef]
19. Alghorani, Y.; Kaddoum, G.; Muhaidat, S.; Pierre, S. On the approximate analysis of energy detection over * rayleigh fading channels through cooperative spectrum sensing. *IEEE Wirel. Commun.* **2015**, *4*, 413–416. [CrossRef]
20. Goodfellow, I.; Bengio, Y.; Courville, A. Deep learning. *arXiv* arXiv:1312.6184v5, 2017.
21. Xie, S.; Girshick, R.; Dollar, P.; Tu, Z.; He, K. Aggregated Residual Transformations for Deep Neural Networks. In Proceedings of the 2017 IEEE Conference on Computer Vision and Pattern Recognition, Honolulu, HI, USA, 21–26 July 2017; pp. 1492–1500.
22. Szegedy, C.; Vanhoucke, V.; Ioffe, S.; Shlens, J.; Wojna, Z. Rethinking the Inception Architecture for Computer Vision. In Proceedings of the IEEE Conference on Computer Vision and Pattern Recognition, Las Vegas, NV, USA, 27–30 June 2016; pp. 2818–2826.
23. 3GPP. Available online: https://portal.3gpp.org/desktopmodules/Specifications/SpecificationDetails.aspx?specificationId=3209 (accessed on 24 June 2019).
24. 3GPP. Available online: https://portal.3gpp.org/desktopmodules/Specifications/SpecificationDetails.aspx?specificationId=3173 (accessed on 10 October 2019).
25. Giambene, G.; Rahman, M.S.; Vinel, A. Analysis of V2V Sidelink Communications for Platoon Applications. In Proceedings of the ICC 2020–2020 IEEE International Conference on Communication (ICC), Dublin, Ireland, 7–11 June 2020.